Nonlinear magneto-plasmonics

Wei Zheng,[1,*] Xiao Liu,[1] Aubrey T. Hanbicki,[2] Berend T. Jonker,[2] and Gunter Lüpke[1]

[1]*Department of Applied Science, College of William & Mary, Williamsburg, VA 23187, USA*
[2]*Materials Science & Technology Division, Naval Research Laboratory, Washington, D.C. 20375, USA*
[*]*wzheng@email.wm.edu*

Abstract: Nonlinear magneto-plasmonics (NMP) describes systems where nonlinear optics, magnetics and plasmonics are all involved. In such systems, nonlinear magneto-optical Kerr effect (nonlinear MOKE) plays an important role as a characterization method, and Surface Plasmons (SPs) work as catalyst to induce many new effects. Magnetization-induced second-harmonic generation (MSHG) is the major nonlinear magneto-optical process involved. The new effects include enhanced MSHG, controlled and enhanced magnetic contrast, etc. Nanostructures such as thin films, nanoparticles, nanogratings, and nanoarrays are critical for the excitation of SPs, which makes NMP an interdisciplinary research field in nanoscience and nanotechnology. In this review article, we organize recent work in this field into two categories: surface plasmon polaritons (SPPs) representing propagating surface plasmons, and localized surface plasmons (LSPs), also called particle plasmons. We review the structures, experiments, findings, and the applications of NMP from various groups.

OCIS codes: (190.2620) Harmonic generation and mixing; (190.4350) Nonlinear optics at surfaces; (240.6680) Surface plasmons; (160.3820) Magneto-optical materials; (230.3810) Magneto-optic systems.

References and links

1. H. Raether, *Surface Plasmons on Smooth and Rough Surfaces and on Gratings* of Springer Tracts in Modern Physics (Springer-Verlag, 1988, Vol. 111).
2. M. I. Stockman, "Nanoplasmonics: past, present, and glimpse into future," Opt. Express **19**(22), 22029–22106 (2011).
3. J. M. Pitarke, V. M. Silkin, E. V. Chulkov, and P. M. Echenique, "Theory of surface plasmons and surface-plasmon polaritons," Rep. Prog. Phys. **70**(1), 1–87 (2007).
4. E. Petryayeva and U. J. Krull, "Localized surface plasmon resonance: Nanostructures, bioassays and biosensing - A review," Anal. Chim. Acta **706**(1), 8–24 (2011).
5. A. Berrier, R. Ulbricht, M. Bonn, and J. G. Rivas, "Ultrafast active control of Localized surface plasmon resonances in silicon bowtie antennas," Opt. Express **18**(22), 23226–23235 (2010).
6. Y. R. Shen, *The Principles of Nonlinear Optics* (Wiley, 1984).
7. R. W. Boyd, *Nonlinear Optics* 3rd ed (Academic, 2008).
8. H. J. Simon, D. E. Mitchell, and J. G. Watson, "Optical second-harmonic generation with surface plasmons in silver films," Phys. Rev. Lett. **33**(26), 1531–1534 (1974).
9. S. I. Bozhevolnyi, J. Beermann, and V. Coello, "Direct observation of localized second-harmonic enhancement in random metal nanostructures," Phys. Rev. Lett. **90**(19), 197403 (2003).
10. C. Anceau, S. Brasselet, J. Zyss, and P. Gadenne, "Local second-harmonic generation enhancement on gold nanostructures probed by two-photon microscopy," Opt. Lett. **28**(9), 713–715 (2003).
11. M. I. Stockman, D. J. Bergman, C. Anceau, S. Brasselet, and J. Zyss, "Enhanced second-harmonic generation by metal surfaces with nanoscale roughness: nanoscale dephasing, depolarization, and correlations," Phys. Rev. Lett. **92**(5), 057402 (2004).
12. T. Y. F. Tsang, "Surface-plasmon-enhanced third-harmonic generation in thin silver films," Opt. Lett. **21**(4), 245–247 (1996).
13. E. M. Kim, S. S. Elovikov, T. V. Murzina, A. A. Nikulin, O. A. Aktsipetrov, M. A. Bader, and G. Marowsky, "Surface-enhanced optical third-harmonic generation in Ag island films," Phys. Rev. Lett. **95**(22), 227402 (2005).
14. S. Palomba and L. Novotny, "Nonlinear excitation of surface plasmon polaritons by four-wave mixing," Phys. Rev. Lett. **101**(5), 056802 (2008).

#245979 Received 16 Jul 2015; revised 10 Sep 2015; accepted 29 Sep 2015; published 19 Oct 2015

15. J. Renger, R. Quidant, N. van Hulst, and L. Novotny, "Surface-enhanced nonlinear four-wave mixing," Phys. Rev. Lett. **104**(4), 046803 (2010).
16. A. V. Krasavin, K. F. MacDonald, N. I. Zheludev, and A. V. Zayats, "High-contrast modulation of light with light by control of surface plasmon polariton wave coupling," Appl. Phys. Lett. **85**(16), 3369–3371 (2004).
17. D. Pacifici, H. J. Lezec, and H. A. Atwater, "All-optical modulation by plasmonic excitation of CdSe quantum dots," Nat. Photonics **1**(7), 402–406 (2007).
18. M. Kauranen and A. V. Zayats, "Nonlinear Plasmonics," Nat. Photonics **6**(11), 737–748 (2012).
19. G. Armelles, A. Cebollada, A. Garcia-Martin, and M. U. Gonzalez, "Magnetoplasmonics: Combining Magnetic and Plasmonic Functionalities," Adv. Opt. Mater. **1**(1), 10–35 (2013).
20. R. F. Pearson, "Application of magneto-optic effects in magnetic materials," Contemp. Phys. **14**(3), 201–211 (1973).
21. M. R. Parker, "The Kerr magneto-optic effect (1876-1976)," Physica B C, **86**, 1171–1176 (1977).
22. C. Hermann, V. A. Kosobukin, G. Lampel, J. Peretti, V. I. Safarov, and P. Bertrand, "Surface-enhanced magneto-optics in metallic multilayer films," Phys. Rev. B **64**(23), 235422 (2001).
23. V. I. Safarov, V. A. Kosobukin, C. Hermann, G. Lampel, J. Peretti, and C. Marlière, "Magneto-optical effects enhanced by surface plasmons in metallic multilayer films," Phys. Rev. Lett. **73**(26), 3584–3587 (1994).
24. B. Sepúlveda, A. Calle, L. M. Lechuga, and G. Armelles, "Highly sensitive detection of biomolecules with the magneto-optic surface-plasmon-resonance sensor," Opt. Lett. **31**(8), 1085–1087 (2006).
25. B. Sepúlveda, P. C. Angelome, L. M. Lechuga, and L. M. Liz-Marzan, "LSRP-based nanobiosensors," Nano Today **4**(3), 244–251 (2009).
26. D. Regatos, D. Farina, A. Calle, A. Cebollada, B. Sepulveda, G. Armelles, and L. M. Lechuga, "Au/Fe/Au multilayer transducers for magneto-optic surface plasmon resonance sensing," J. Appl. Phys. **108**(5), 054502 (2010).
27. Z. Yu, G. Veronis, Z. Wang, and S. Fan, "One-way electromagnetic waveguide formed at the interface between a plasmonic metal under a static magnetic field and a photonic crystal," Phys. Rev. Lett. **100**(2), 023902 (2008).
28. B. Sepulveda, L. M. Lechuga, and G. Armelles, "Magnetooptic effects in surface-plasmon-plaritons slab waveguides," J. Lightwave Technol. **24**(2), 945–955 (2006).
29. V. V. Temnov, G. Armelles, U. Woggon, D. Guzatov, A. Cebollada, A. Garcia-Martin, J. Garcia-Martin, T. Thomays, A. Leitenstorfers, and R. Bratschitschs, "Active magneto-plasmonics in hybrid metal–ferromagnet structures," Nat. Photonics **4**(2), 107–111 (2010).
30. A. Kirilyuk and T. Rasing, "Magnetization-induced second harmonic generation," in *Handbook of Magnetism and Advanced Magnetic Materials* (John Wiley & Sons, Ltd. 2007, Volume 3: Novel Techniques for Characterizing and Preparing Samples).
31. V. K. Valev, A. Kirilyuk, F. Dalla Longa, J. T. Kohlhepp, B. Koopmans, and Th. Rasing, "Observation of periodic oscillations in magnetization-induced second harmonic generation at the Mn/Co interface," Phys. Rev. B **75**(1), 012401 (2007).
32. Y. Fan, K. J. Smith, G. Lüpke, A. T. Hanbicki, R. Goswami, C. H. Li, H. B. Zhao, and B. T. Jonker, "Exchange bias of the interface spin system at the Fe/MgO interface," Nat. Nanotechnol. **8**(6), 438–444 (2013).
33. M. Fiebig, D. Fröhlich, B. B. Krichevtsov, and R. V. Pisarev, "Second harmonic generation and magnetic-dipole-electric-dipole interference in antiferromagnetic Cr2O3," Phys. Rev. Lett. **73**(15), 2127–2130 (1994).
34. G. Tessier, C. Malouin, P. Georges, A. Brun, D. Renard, V. V. Pavlov, P. Meyer, J. Ferre, and P. Beauvillain, "Magnetization-induced second-harmonic generation enhanced by surface plasmons in ultrathin Au/Co/Au metallic films," Appl. Phys. B **68**(3), 545–548 (1999).
35. G. Tessier and P. Beauvillain, "Non linear optics and magneto-optics in ultrathin metallic films," Appl. Surf. Sci. **164**(1-4), 175–185 (2000).
36. A. V. Kosobukin, "On the theory of near-field magneto-optical microscopy via plasmonic modes of nanowire," Tech. Phys. Lett. **37**(4), 387–390 (2011).
37. J. Pistora, M. Lesnak, and O. Vlasin, "Surface plasmon resonance sensor with Magneto-Optical thin film," Acta Electrotechnica et Informatica **10**, 19–21 (2010).
38. W. Zheng, A. T. Hanbicki, B. T. Jonker, and G. Lüpke, "Surface Plasmon-enhanced Transverse Magnetic Second-Harmonic Generation," Opt. Express **21**(23), 28842–28848 (2013).
39. W. Zheng, A. T. Hanbicki, B. T. Jonker, and G. Lüpke, "Control of magnetic contrast with nonlinear magneto-plasmonics," Sci. Rep. **4**, 6191 (2014).
40. C. Daboo, R. J. Hicken, D. E. P. Eley, M. Gester, S. J. Gray, A. J. R. Ives, and J. A. C. Bland, "Magnetization reversal processes in epitaxial Fe/GaAs(001) films," Appl. Phys. Lett. **75**, 5586 (1994).
41. R. P. Cowburn, S. J. Gray, J. Ferre, J. A. C. Bland, and J. Miltat, "Magnetic switching and in-plane uniaxial anisotropy in ultrathin Ag/Fe/Ag(100) epitaxial films," Appl. Phys. Lett. **78**, 7210 (1995).
42. C. Daboo, R. J. Hicken, E. Gu, M. Gester, S. J. Gray, D. E. P. Eley, E. Ahmad, J. A. Bland, R. Ploessl, and J. N. Chapman, "Anisotropy and orientational dependence of magnetization reversal processes in epitaxial ferromagnetic thin films," Phys. Rev. B Condens. Matter **51**(22), 15964–15973 (1995).
43. D. M. Newman, M. L. Wears, R. J. Matelon, and D. Mchugh, "Non-linear optics and magneto-optics on nano-structured interfaces," Appl. Phys. B **74**(7-8), 719–722 (2002).
44. D. M. Newman, M. L. Wears, and R. J. Matelon, "Plasmon enhanced magneto-optic behaviour in the linear and non-linear optical fields," J. Magn. Magn. Mater. **242-245**, 980–983 (2002).

#245979 Received 16 Jul 2015; revised 10 Sep 2015; accepted 29 Sep 2015; published 19 Oct 2015

45. I. Razdolski, S. Parchenko, A. Stupakiewicz, S. Semin, A. Stognij, A. Maziewski, A. Kirilyuk, and T. Rasing, "Second-harmonic generation from a magnetic buried interface enhanced by an interplay of surface plasma resonances," ACS Photonics **2**(1), 20–26 (2015).
46. I. Razdolski, D. G. Gheorghe, E. Melander, B. Hjorvarsson, P. Patoka, A. V. Kimel, A. Kirilyuk, E. T. Papaioannou, and T. Rasing, "Nonlocal nonlinear magneto-optical response of a magnetoplasmonic crystal," Phys. Rev. B **88**(7), 075436 (2013).
47. R. K. Chang, J. Ducuing, and N. Bloembergen, "Relative phase measurement between fundamental and second-harmonic light," Phys. Rev. Lett. **15**(1), 6–8 (1965).
48. E. Schwarzberg, G. Berkovic, and G. Marowsky, "Nonlinear interferometry and phase measurements for surface second-harmonic generation in a dispersive geometry," Appl. Phys., A Mater. Sci. Process. **59**(6), 631–637 (1994).
49. K. Sato, A. Kodama, M. Miyamoto, A. V. Petukhov, K. Takanashi, S. Mitani, H. Fujimori, A. Kirilyuk, and T. Rasing, "Anisotropic magnetization-induced second harmonic generation in Fe/Au superlattices," Phys. Rev. B **64**(18), 184427 (2001).
50. A. Kirilyuk, G. M. H. Knippels, A. F. G. Meer, S. Renard, Th. Rasing, I. R. Heskamp, and J. C. Lodder, "Observation of strong magnetic effects in visible-infrared sum frequency generation from magnetic structures," Phys. Rev. B **62**(2), 783–786 (2000).
51. V. L. Krutyanskiy, A. L. Chekhov, V. A. Ketsko, A. I. Stognij, and T. V. Murzina, "Giant nonlinear magneto-optical response of magnetoplasmonic crystals," Phys. Rev. B **91**(12), 121411 (2015).
52. A. L. Chekhov, V. L. Krutyanskiy, A. N. Shaimanov, A. I. Stognij, and T. V. Murzina, "Wide tunability of magnetoplasmonic crystals due to excitation of multiple waveguide and plasmon modes," Opt. Express **22**(15), 17762–17768 (2014).
53. V. I. Belotelov, L. E. Kreilkamp, I. A. Akimov, A. N. Kalish, D. A. Bykov, S. Kasture, V. J. Yallapragada, A. Venu Gopal, A. M. Grishin, S. I. Khartsev, M. Nur-E-Alam, M. Vasiliev, L. L. Doskolovich, D. R. Yakovlev, K. Alameh, A. K. Zvezdin, and M. Bayer, "Plasmon-mediated magneto-optical transparency," Nat. Commun. **4**, 2128 (2013).
54. T. V. Murzina, T. V. Misuryaev, A. F. Kravets, J. Gudde, D. Schuhmacher, G. Marowsky, A. A. Nikulin, and O. A. Aktsipetrov, "Nonlinear magneto-optical Kerr effect and plasmon-asisted SHG in magnetic nanomaterials exhibiting giant magnetoresistance," Surf. Sci. **482–485**, 1101–1106 (2001).
55. O. Aktsipetrov, T. V. Murzina, E. M. Kim, R. V. Kapra, A. A. Fedyanin, M. Inoue, A. F. Kravets, S. V. Kuznetsova, M. V. Ivanchenko, and V. C. Lifshits, "Magnetization-induced second- and third- harmonic generation in magnetic thin films and nanoparticles," J. Opt. Soc. Am. B **22**(1), 138–147 (2005).
56. O. Aktsipetrov, T. V. Dolgova, A. A. Fedyanin, T. V. Murzina, M. Inoue, K. Nishimura, and H. Uchida, "Magnetization-induced second- and third- harmonic generation in magnetophotonic crystals," J. Opt. Soc. Am. B **22**(1), 176–185 (2005).
57. T. V. Murzina, I. A. Kolmychek, J. Wouters, T. Verbiest, and O. A. Aktsipetrov, "Plasmon-assisted enhancement of third-order nonlinear optical effects in core(shell) nanoparticles," J. Opt. Soc. Am. B **29**(1), 138–143 (2012).
58. V. K. Valev, A. V. Silhanek, W. Gillijns, Y. Jeyaram, H. Paddubrouskaya, A. Volodin, C. G. Biris, N. C. Panoiu, B. De Clercq, M. Ameloot, O. A. Aktsipetrov, V. V. Moshchalkov, and T. Verbiest, "Plasmons reveal the direction of magnetization in nickel nanostructures," ACS Nano **5**(1), 91–96 (2011).
59. V. K. Valev, A. V. Silhanek, N. Verellen, W. Gillijns, P. Van Dorpe, O. A. Aktsipetrov, G. A. E. Vandenbosch, V. V. Moshchalkov, and T. Verbiest, "Asymmetric Optical Second-Harmonic Generation from Chiral G-Shaped Gold Nanostructures," Phys. Rev. Lett. **104**(12), 127401 (2010).
60. V. K. Valev, N. Smisdom, A. V. Silhanek, B. De Clercq, W. Gillijns, M. Ameloot, V. V. Moshchalkov, and T. Verbiest, "Plasmonic Ratchet Wheels: Switching Circular Dichroism by Arranging Chiral Nanostructures," Nano Lett. **9**(11), 3945–3948 (2009).
61. J. B. Pendry, "A Chiral Route to Negative Refraction," Science **306**(5700), 1353–1355 (2004).
62. S. Zhang, Y. S. Park, J. Li, X. Lu, W. Zhang, and X. Zhang, "Negative Refractive Index in Chiral Metamaterials," Phys. Rev. Lett. **102**(2), 023901 (2009).
63. E. Plum, J. Zhou, J. Dong, V. A. Fedotov, T. Koschny, C. M. Soukoulis, and N. I. Zheludev, "Metamaterial with Negative Index Due to Chirality," Phys. Rev. B **79**(3), 035407 (2009).

1. Introduction

Surface plasmons (SPs) consist of coherent delocalized electrons that exist at the interface between a metal and a dielectric [1–3]. Two types of SPs are commonly studied. One consists of propagating plasmons, or surface plasmon polariton (SPP), which can be excited by photons with a prism or a grating as a coupler to match the wave vectors of photon and surface plasmon. The other is a localized surface plasmon (LSP) which can be excited by photons absorbed by nanoparticles with sizes comparable or smaller than the wavelength of the photons. Both types of SPs have the same significant effect: the electromagnetic (EM) field is greatly enhanced at the surface where SPs are excited [3–5].

#245979 Received 16 Jul 2015; revised 10 Sep 2015; accepted 29 Sep 2015; published 19 Oct 2015

The field enhancement effect of SPs is very favorable to nonlinear optical (NLO) processes, which are inherently very weak. SPs can boost parametric nonlinearity processes mainly in two ways. The first one is that the plasmon-enhanced electric field ***E(ω)*** boosts the polarization ***P***, described in the electric-dipole approximation by Eq. (1):

$$P(\omega, 2\omega, ...) = \chi^{(1)} E(\omega) + \chi^{(2)} E(\omega) E(\omega) + ... \quad (1)$$

where $\chi^{(1)}$ is the linear optical susceptibility tensor and $\chi^{(2)}$ is the second-order nonlinear susceptibility tensor, which gives rise to second-harmonic generation (SHG), taking into account that the 4th-rank susceptibility tensor representing the quadrupolar contributions is much smaller. SHG is only allowed in media without inversion symmetry because it is an even-order ($\chi^{(2)}$) NLO effect. Therefore, SHG can be generated only in noncentrosymmetric media or at surfaces or interfaces between centrosymmetric media where the inversion symmetry is broken [6,7]. This is the second way that SPs can boost parametric nonlinearites: SHG is generated at surfaces or interfaces, the same region where SPs are excited and the enhanced field is strongest. Plasmon-enhanced SHG has been reported first by Simon *et al*. on silver films [8]. Later studies have shown SPs-enhanced SHG in other materials [9–11], SPs-enhanced THG [12,13], and four wave mixing [14,15] in various structures.

Plasmon-induced effects on the nonlinear index, which is another branch of NLO processes, are also being studied. The interesting applications include: all optical switching and modulation in plasmonic wave-guides, controlling light with light in plasmonic nanostructures, etc [16–18]. The terminology "nonlinear plasmonics" is adopted to describe systems where SPs and NLO processes co-exist as mentioned above [18].

Another topic, where SPs are highly involved, is magneto-plasmonics (MP), which describes systems where SPs and magnetic features coexist [19]. The studies in MP fall into two main categories: SPs' effect on magneto-optical (MO) activities [20], and magnetic field tuning of SPs. MO activities, especially magneto-optical Kerr effect (MOKE) [21], play important role in both categories. For the former one, Eq. (2) briefly describes how SPs affect the MO activities through the enhanced field:

$$\left| r_{ps} \right| \propto \left\langle E_p E_s \right\rangle d \left| \varepsilon_{mo} \right| \quad (2)$$

where r_{ps} is the MO polarization conversion, which determines the *Kerr* rotation, ε_{mo} is MO constant of the material, d is the thickness of the thin layer MO material. E_p and E_s are the component of p and s polarization field in the MO material [19,22]. The MOKE response is boosted by the SPs-enhanced field. The first experimental study of this effect has been reported by Safarov *et al*. on metallic multilayer films [23]. Later on, the studies have been expanded to ferromagnetic metal nanoparticles (including nanowires, nanodiscs, etc.), noble metal-ferromagnetic nanoparticles, noble metal nanoparticles and ferromagnetic dielectric layers, perforated continuous layers, etc [19]. with applications for bio-chemical sensors [24–26] and optical isolators and modulators [27,28]. For the second category of studies in MP, the magnetic field exerts an influence on the SPs by modulating SPs' wave vector through MO constant ε_{mo}, which is a function of the applied magnetic field [19]. The major application of this effect is active plasmon wavevector modulation [29].

In this paper, we review the interdisciplinary studies at the intersection of Nonlinear Plasmonics (NP) and Magneto-Plasmonics (MP), referred to as Nonlinear Magneto-Plasmonics (NMP). NMP adopts nonlinear MOKE, especially magnetization-induced second-harmonic generation (MSHG) [30] as a research tool. MSHG is more surface sensitive than the linear optical MOKE, because it is sensitive to the interface or surface magnetization where the symmetry is broken [6,7,30,31]. On the other hand, compared to metal surface second-harmonic generation (SHG) in NP, MSHG contains nonzero magnetic components of the second-order nonlinear susceptibility tensor which makes MSHG extremely sensitive to

#245979 Received 16 Jul 2015; revised 10 Sep 2015; accepted 29 Sep 2015; published 19 Oct 2015

subtle modifications of the spin-polarized electronic structure of transition metal surfaces [32,33], the same region where SPs are present. Hence, NMP combines the strength and unique features of NP and MP. The studies are classified according to the types of SPs into two categories: SPP and LSP.

2. Nonlinear magneto-plasmonics with surface plasmon polaritons

The first NMP experimental study was carried out by Tessier *et al.* in 1999 [34,35]. The measurements were done using the attenuated total reflection (ATR) technique in the Kretschmann geometry [1] [Fig. 1(a)]. For light incident in the x-z plane [Fig. 1(b)], the longitudinal, transverse, and polar MSHG are classified according to the direction of magnetization component parallel to the x, y, and z-axis, respectively [30]. Both transverse (T) and longitudinal (L) MSHG were studied on an Au (25 μm thick) / Co (3 μm thick) / Au (3 μm thick) / air system.

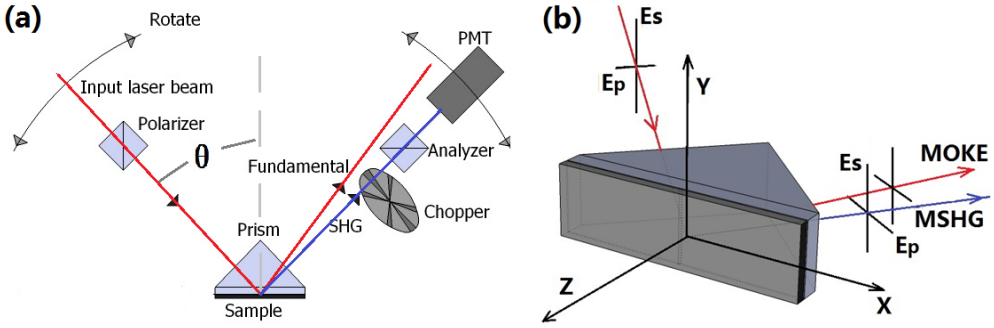

Fig. 1. (a) Kretschmann geometry for SPP excitation in NMP, and (b) coordinate system for MSHG. Red lines represent the fundamental beam, which is normally generated by a Titanium doped Sapphire laser, with a wavelength of around 800 nm. Blue lines represent the double frequency beam with a wavelength of about 400 nm. (adapted from Ref. [38])

In the coordinate system depicted by Fig. 1(b), the nonlinear susceptibility tensors for L- and T-MSHG are derived with proper simplification by symmetry as [30]

$$\chi_{ijk}^{(L)} = \begin{pmatrix} 0 & 0 & 0 & 0 & \chi_{xzx}^{even} & \chi_{xyx}^{odd} \\ \chi_{yxx}^{odd} & \chi_{yyy}^{odd} & \chi_{yzz}^{odd} & \chi_{yzy}^{even} & 0 & 0 \\ \chi_{zxx}^{even} & \chi_{zyy}^{even} & \chi_{zzz}^{even} & \chi_{zyz}^{even} & 0 & 0 \end{pmatrix} \tag{3}$$

and

$$\chi_{ijk}^{(T)} = \begin{pmatrix} \chi_{xxx}^{odd} & \chi_{xyy}^{odd} & \chi_{xzz}^{odd} & 0 & \chi_{xzx}^{even} & 0 \\ 0 & 0 & 0 & \chi_{yzy}^{even} & 0 & \chi_{yxy}^{odd} \\ \chi_{zxx}^{even} & \chi_{zyy}^{even} & \chi_{zzz}^{even} & 0 & \chi_{zxz}^{odd} & 0 \end{pmatrix}, \tag{4}$$

where odd terms change signs with magnetization reversal and thus exhibit the switching process, while the even terms are not sensitive to magnetization and are considered as crystal contribution. Knowing the polarization of the incident beam, the second-order nonlinear optical polarization can be calculated by the tensors.

In Tessier's study, a second-harmonic signal (includes MSHG and SHG) enhanced by a factor of four was observed. The most interesting result of this study is the sign reversal effect of the magnetic contrast near the SP resonance [Fig. 2] . The magnetic contrast can be defined as

#245979 Received 16 Jul 2015; revised 10 Sep 2015; accepted 29 Sep 2015; published 19 Oct 2015

$$C = \frac{I^{(2\omega)}(+M) - I^{(2\omega)}(-M)}{I^{(2\omega)}(+M) + I^{(2\omega)}(-M)}, \tag{5}$$

where *I(+ M)* and *I(-M)* are intensities for the two magnetization states. The reversal effect refers to the change of the signs of magnetic contrast *C*. That means the value of *I(+ M)* and *I(-M)* has a drastic change at about 44° incident angle, where the SHG signal has a strong minimum.

A model on the basis of a nonlocal field theory [36] was developed to explain the sign reversal effect. The nonlinear susceptibility is assumed to be nonlocal in *z* direction. Following this approach, as a result of self-consistent solutions of the wave equations the fundamental electric fields of the light are continuous functions, which can be calculated on the basis of the Green's functions for the interfaces of trilayer films. Taking into account multiple interference of different contributions, the total nonlinear electric field was calculated numerically. This model allows to distinguish the contributions of the various interfaces to SHG, and agrees with the experimental data very well.

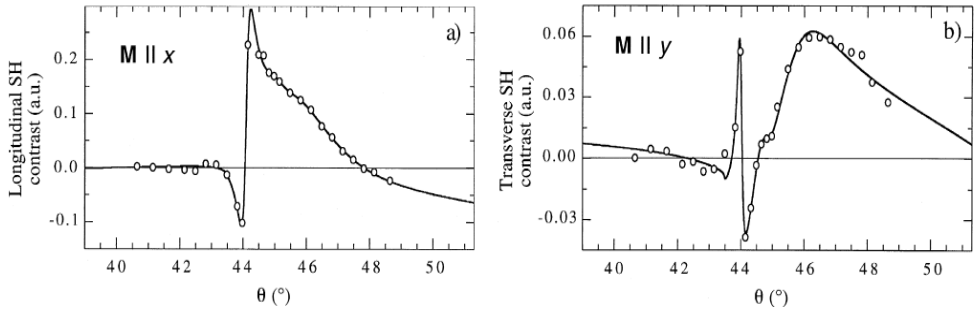

Fig. 2. Longitudinal and transverse magnetic contrasts of MSHG as a function of the incident angle, the signs of magnetic contrast change drastically at about 44°, the open dots are measured values, the curves represent best fits. (adapted from Ref. [35])

Historically, one dilemma for MP systems is that the noble metal layer supports high quality SP, but a very large magnetic field (several Tesla) is needed to achieve MO activity. On the other hand, the ferromagnetic (FM) layer exhibits large MO activity, which makes it possible to make real MO devices. However, the huge losses in the FM layer causes an overdamping of plasmon resonance, and thus impairs the strength of SP. The prevailing configuration, noble metal/FM/noble metal heterostructures [23–26,29,34,35,37], combines the strength of good quality SP and large MO effect, but makes the structure complex and separates the source of SP and magnetization which compromises the coupling between them.

Taking the advantage of the spatial overlap of SPP and MSHG source, a simpler structure, 10-nm thick single-crystal Fe film (grown on an MgO (001) substrate with axis [110] along the x-direction), was adopted by Zheng *et al.* [38]. Large enhancement of the MSHG signal intensity was observed under ATR [Fig. 3(a)]. A comparison between the contrast ratio of SPP-enhanced MOKE and MSHG signal shows NMP has much more pronounced effect over MP [Fig. 3(b)]. Figure 3(b) shows a continuously enhanced contrast ratio for T-MSHG over a large range of incident angle. The results suggest that as an inherent surface sensitivity technique, MSHG would be ideally paired with SPs for sensing applications.

#245979 Received 16 Jul 2015; revised 10 Sep 2015; accepted 29 Sep 2015; published 19 Oct 2015

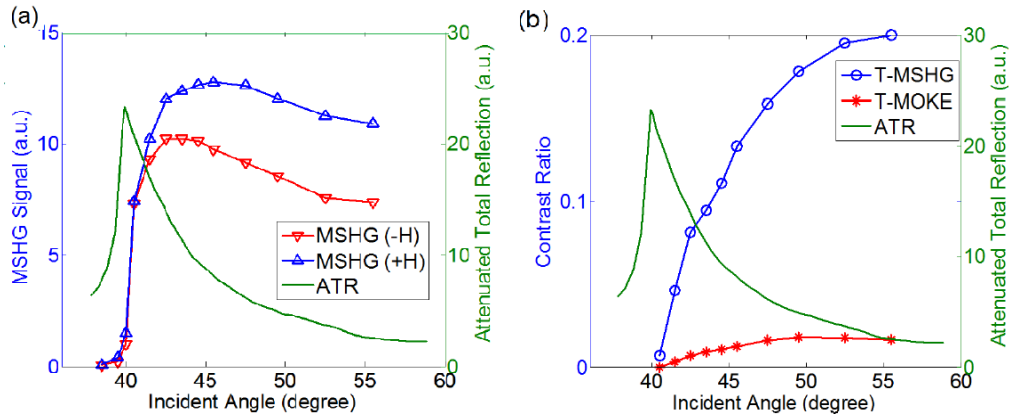

Fig. 3. (a) Enhanced signal strength of transverse MSHG as a function of the incident angle on 10-nm thick Fe thin film sample, and (b) comparison of SPP-enhanced magnetic contrast of MSHG and MOKE. The ATR curve (green) is shown as reference. (adapted from Ref. [38])

Note that the ATR curve for this pure Fe film is not as sharp as that of noble metals as it is stretched out due to absorption, i.e. strong damping. The simple structure makes the analysis easier. The experimental ATR curve agrees with the calculated one very well. The trend of MSHG values as a function of incident angle in Fig. 3(a) is very similar to a calculated curve, if one of the nonlinear susceptibility tensors χ_{xzz}^{odd} dominates over others. This indicates that there exists a great anisotropy in the second-order susceptibility tensor of T-MSHG and its expression can be simplified.

A further study on the same system reveals a strong control effect of SPs on the magnetic contrast [39]. Due to the cubic magnetic anisotropy, single-crystalline iron film has four magnetization states [40–42]. The magnetic contrast between these states can be varied over a wide range with the presence of SPs [Fig. 4]. The magnetic contrast of transverse and longitudinal MSHG display opposite trends, which originates from the change of relative phase between MSHG components caused by SPs. Such a system enables simultaneous investigation of both longitudinal and transverse magnetization components regardless of the external magnetic field. This study has potential usage in quaternary magnetic storage systems because it enables the read-out of all four magnetization states from crystalline iron with high contrast ratio.

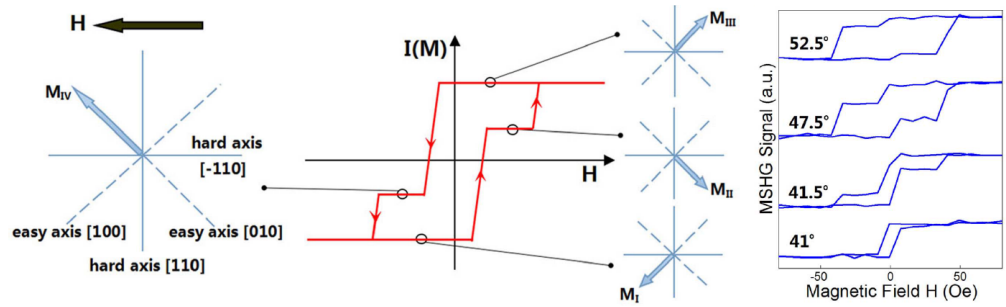

Fig. 4. As a magnetically anisotropic material, crystalline Fe has four magnetization states. With the help of SPs, MSHG technique can read out all four magnetization states with good magnetic contrast, the longitudinal and transverse MSHG can be studied simultaneously. The hysteresis loops on the right reveal the control effect of magnetic contrast with NMP. (adapted from Ref. [39])

Newman *et al*. studied enhancement of MSHG by grating-excited SPs [43,44], in which the sharp drop of reflectance from gratings indicates the optical energy being converted from

#245979 Received 16 Jul 2015; revised 10 Sep 2015; accepted 29 Sep 2015; published 19 Oct 2015

the incident beam to plasmon generation. An enhanced SHG and fractional intensity change (similar concept to magnetic contrast) are observed on a nickel grating used in optical disk manufacture with a period of 1200 nm and a profile depth of 70 nm.

The group of Kirilyuk and Rasing adopted a more complex grating structure, 100 × 100 μm array of 120 nm thick Au stripes deposited on 4 μm thick (Bi, Tm) iron garnet (BTIG) grown on gallium gadolinium garnet (GGG) substrate [45]. Through systematic measurements as a function of SPs excitation wavelength and angle of incidence, it is demonstrated that at an optimized condition SPs can be excited at both Au/air and Au/(Bi, Tm) interface, which is buried beneath Au stripes. Furthermore, the MSHG is enhanced at Au/(Bi, Tm) interface despite the very thick 120 nm Au layer [Fig. 5]. This finding is appealing for MP device manufacture. This study also pointed out the future direction and application could reside in an optical control of the MP properties and ultrafast nonlinear plasmonics.

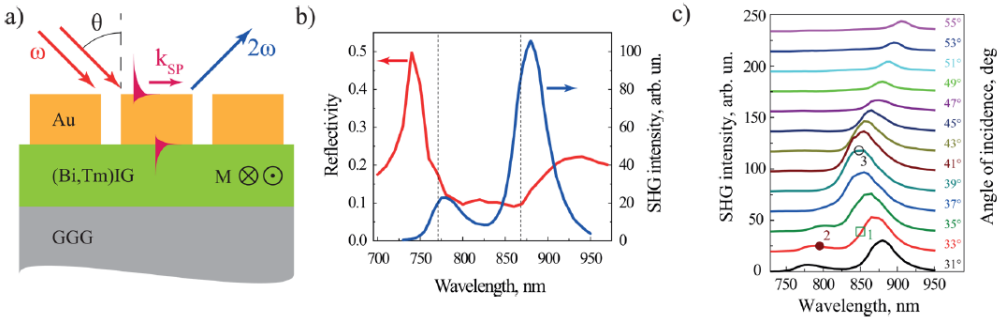

Fig. 5. (a) Au/BTIG/GGG grating structures, (b) at 31° incidence, wavelength dependence of reflectivity and SHG intensity. Vertical dashed lines indicate the spectral positions of SPs at two interfaces, and (c) SHG intensity as a function of wavelength and angle of incidence, point 1 and 2 indicate the conditions where SPs at each interface are excited, respectively, point 3 indicates the condition that SPs are excited at both interfaces. (adapted from Ref. [45])

The same group also conducted NMP research on an Au(2 nm)/Co(60 nm)/Ti(2 nm)/Si(111) plasmonic crystal [46]. In this system, the Au and Co layers were decorated with a hexagonal array of circular holes of average diameter of 250 nm and average pitch size of 470 nm. The authors provided profound discussion on the effect of SPs on MSHG. The enhanced MSHG strength and magnetic contrast is observed in the vicinity of the SPs. Direct phase measurements using the nonlinear interferometry method [47,48] show that the change of magnetic contrast originates from the change of phase between magnetic and nonmagnetic MSHG contributions [Fig. 6]. The activation of a nonlocal quadrupole mechanism [18,49] of the MSHG by SPs was attributed to such phase change.

In earlier time, the group of Kirilyuk and Rasing also reported strong magnetization induced changes of the infrared-visible sum-frequency generation (SFG) intensity from thin magnetic films using a free electron laser. The reported effect occurs with the help of the SPs excited by magnetic grating made from Pt/CoNi/Pt sandwich [50].

#245979 Received 16 Jul 2015; revised 10 Sep 2015; accepted 29 Sep 2015; published 19 Oct 2015

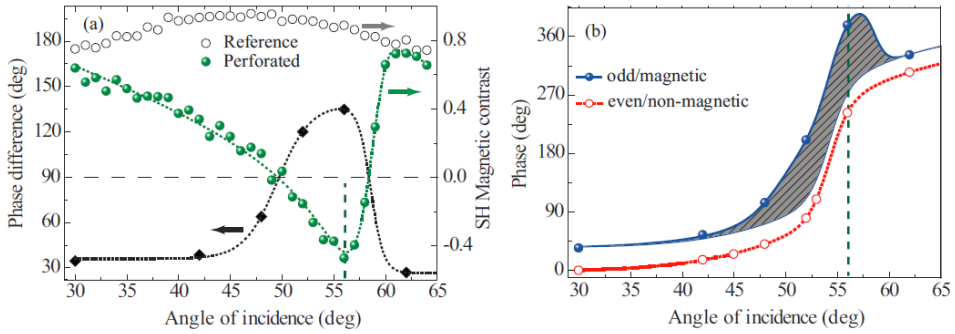

Fig. 6. (a) SHG magnetic contrast as a function of incident angle for the reference (empty dots) and perforated (green full dots) films. Black diamonds represent the phase difference between even and odd (refer to Eq. (3) and (4)) magnetic SHG contributions, (b) relative phases of the even (red empty dots) and odd (blue full dots) SHG components. The dashed area represents phase shift introduced by the SPPs. Dotted lines are the result of an interpolation. The vertical line refers to the SP resonant angle. (adapted from ref. 46)

A very recent NMP study on grating structures has been reported by the group of Murzina [51]. A grating with a period of d = 730 nm is formed by 40-nm thick gold film stripes covering a 2-μm thick bismuth iron garnet (BIG) layer on a gadolinium gallium garnet (GGG) substrate. Such structure is called a magneto-plasmonic crystal (MPC). In this study, both the SPPs at metal/dielectric interfaces and the waveguide modes [52,53] in the dielectric slab contribute to the field enhancement. Besides the phase modulation by the SPP, a strong modulation of the SHG intensity by both SPPs and the waveguide modes is observed. The field enhancement contributed by multi-sources shows an unique feature of properly designed MPCs [Fig. 7]. This study is very attractive for potential applications of the MPC structures as magnetic field active modulator.

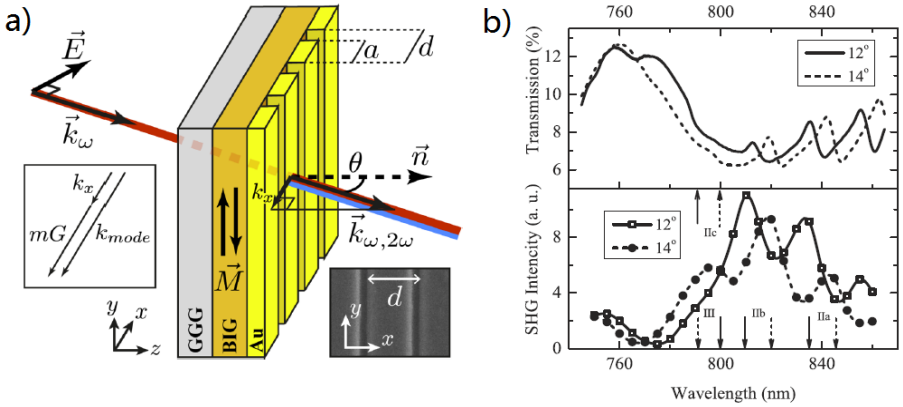

Fig. 7. (a) The grating structure is also called magneto -plasmonic crystal, a transmission geometry is used to excite SPP and generate SHG. A dc magnetic field is applied parallel to the stripes to control the light flow, (b) Wavelength dependent transmission and SHG intensity indicate both SPPs and waveguide modes contribute to the SHG. IIa, IIb and IIc indicate the waveguide modes, and III indicate the SPP. (adapted from ref. 51)

3. Nonlinear magneto-plasmonics with localized surface plasmons

The first localized surface plasmons (LSPs)' effect on MSHG has been reported by the group of Murzina in 2001 [54]. Wavelength-dependent MSHG measurements of Co_xAg_{1-x} and $(CoFe)_x(Al2O3)_{1-x}$ nano-granular film show pronounced LSP resonances in the vicinity of 620 to 640 nm, where the second-harmonic signal is strongest. The effect of component weight x on LSP-enhanced MSHG and magnetic contrast for the above two materials is also studied

#245979 Received 16 Jul 2015; revised 10 Sep 2015; accepted 29 Sep 2015; published 19 Oct 2015

[Fig. 8]. A later paper reported magnetic induced third-harmonic generation (THG) in the same system [55]. Good agreement between the observed LSPs resonances and numerical calculations confirmed the LSPs' effect on magnetization-induced SHG and THG. The authors suggest the excitation of LSPs play an important role in the correlation between giant magnetroresistance (GMR) and MSHG.

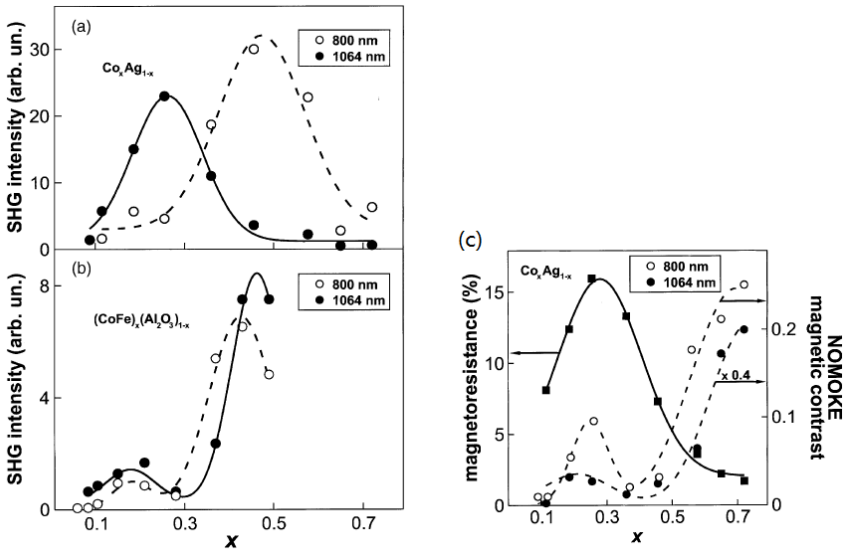

Fig. 8. (a)(b) MSHG intensity as a function of x. x is the weight of element for Co_xAg_{1-x} and $(CoFe)_x(Al2O3)_{1-x}$ nano-granular films at the fundamental wavelengths of 1064 nm and 800 nm, (c) MSHG magnetic contrast and magnetoresistance as a function of x for Co_xAg_{1-x}. (adapted from Ref. [54])

The same group also reported studies of NMP on Fe_2O_3(Au) nanoparticles, Au/Co/Au nanosandwiches, magnetophotonic microcavities (MMCs) and magnetophotonic crystals. Plasmon-assisted modifications of magneto-optical response and magnetization-induced SHG and THG were studied [56,57].

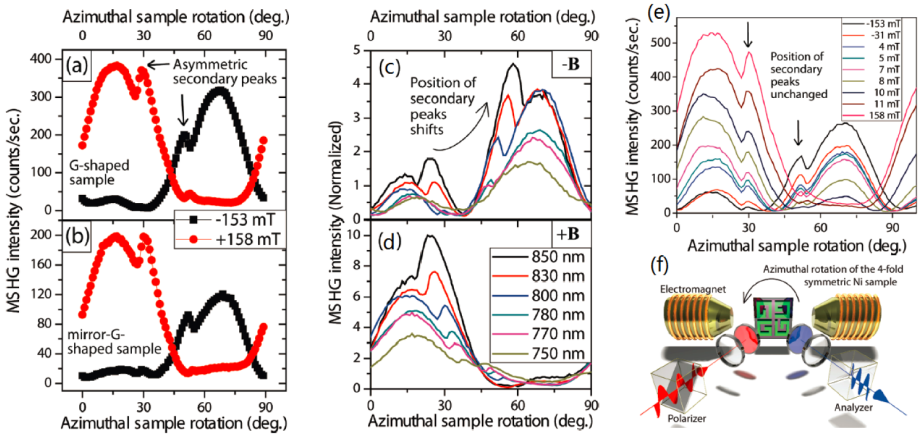

Fig. 9. (a)(b)MSHG intensities as a function of azimuthal sample rotation angle show asymmetric secondary peaks, (c)(d) the position of secondary peaks changes with wavelength, while the structure remain same, which excludes the structure anisotropy as the origin of the asymmetry, (e) the position of the secondary peaks remains unaffected with different magnetic field applied, which excludes the magnetic field as the origin, (f) the four-fold symmetric sample and experimental setup. (adapted from Ref. [58])

#245979 Received 16 Jul 2015; revised 10 Sep 2015; accepted 29 Sep 2015; published 19 Oct 2015

Valev *et al*. studied MSHG on G-shape nickel nanostructure with a four-fold in plane symmetry [58]. MSHG signals are also expected to have four-fold symmetry [59] because it is a symmetry sensitive technique. Surprisingly, besides the four-fold symmetry main peaks of MSHG signal enhanced by LSPs, there appear secondary peaks, which make the whole response asymmetric [Fig. 9]. By excluding the magnetic field, surface anisotropy, diffraction induced wavelength independence, the sides of the G-shape nanostructures, or a shift of the plasmon resonance caused by angle-of-incidence structure, the authors suggest a magneto-chiral effect [60–63] as the reason for the asymmetry. The plasmonic and nonlinear optical response are tuned by such effect. This study shows a novel way in NMP to combine nanophotonics, nanoelectronics and nanomagnetics. Since chirality can lead to negative refractive index, a device that can switch the sign of refractive index with magnetic field is proposed.

4. Conclusion and perspectives

We have reviewed the studies in nonlinear magneto-plasmonics (NMP), from the experiments, structures, scientific findings to possible applications. Many interesting effects are revealed (Table 1).

Table 1. Comparison of different NMP structures

Structure	Features and findings
Au/Co/Au multi-layer	ATR geometry, enhanced MSHG, magnetic contrast sign reversal effect
Pure iron layer	ATR geometry, simple structure, stretched ATR curve, enhanced MSHG, magnetic contrast control effect
Pure nickel grating	Reflection geometry, sharp drop of reflectance indicates the SPs, enhanced MSHG, enhanced magnetic contrast
Au stripes deposited on (Bi, Tm) iron garnet (BTIG)	Reflection geometry, SPs can be excited at both Au/air and Au/(Bi, Tm) interfaces, MSHG can be enhanced at burried Au/(Bi, Tm) interface
Au/Co layer with periodic holes on Ti layer	Reflection geometry, enhanced MSHG, enhanced magnetic contrast, phase change between magnetic and nonmagnetic MSHG contributions in the vicinity of the SPs
Gold film stripes on bismuth iron garnet (BIG) layer	Transmission geometry, both SPPs and waveguide modes contribute to the enhanced SHG
Co_xAg_{1-x} and $(CoFe)_x(Al2O3)_{1-x}$ nano-granular film	Reflection geometry, the weight of element x has effect on SHG intensity, MSHG magnetic contrast and magnetroresistance, LSPs is important to the correlation between giant magnetroresistance (GMR) and MSHG.
G-shape nickel nanostructure	Reflection geometry, second harmonic microscopy shows plasmonic local field enhancements, magneto-chiral effect

We propose the future studies of NMP will reside in the following three major directions: 1) development of NMP devices with real applications; 2) effects of other techniques on NMP, for example, the temporal study by pump-probe technique; 3) active control of one element by the other, for example, MSHG surveys the control of magnetization by SPs at the interface.

Acknowledgments

The optical experiments performed at the College of William and Mary are supported by the Department of Energy through Grant No. DE-FG02-04ER46127. The sample growth at NRL is supported by core programs at NRL and the NRL Nanoscience Institute.

#245979 Received 16 Jul 2015; revised 10 Sep 2015; accepted 29 Sep 2015; published 19 Oct 2015